

Supporting Information

In-operando dipole orientation for bipolar injection from air-stable electrodes into organic semiconductors

Anton Kirch^{1*}, Joan Ràfols-Ribé¹, Yuntao Qiu¹, Thushar Salkod Mahabaleshwar^{1,3}, William Strömberg¹, Ajay Kumar Poonia^{1,2,3}, Preetam Dacha¹, Kumar Saumya¹, Sri Harish Kumar Paleti^{1,3}, Christian Larsen¹, Nicolò Maccaferri^{2,3}, and Ludvig Edman^{1,3}

¹ The Organic Photonics and Electronics Group, Department of Physics, Umeå University, SE-90187 Umeå, Sweden

² Ultrafast Nanoscience Group, Department of Physics, Umeå University, SE-90187 Umeå, Sweden

³ Wallenberg Initiative Materials Science for Sustainability, Department of Physics, Umeå University, SE-90187 Umeå, Sweden

* Correspondence: anton.kirch@umu.se

Table of contents

S1. Cyclic voltammetry measurements	2
S2. Voltage-luminance turn-on transients.....	3
S3. Capacitance density	4
S4. Equivalent circuit model (ECM) parameters.....	5
S5. Further polar molecules as dopants	6
S6. Using the TADF emitter 4TCzBN instead of SY.....	8
S7. Further impedance spectroscopy under bias	9

S1. Cyclic voltammetry measurements

We perform cyclic voltammetry (CV) measurements to extract the energy levels of Super Yellow and TMPE-OH on a Metrohm PGSTAT302 using a standard electrochemical cell at a scan rate of 50 mV/s. Super Yellow's CV is measured with a thin film of SY on gold-coated glass electrodes as the working electrode (WE). The thin films are prepared through spin coating an 8 g/L solution in cyclohexanone at 2000 rpm (2000 rpm/s acceleration) for 60 s and annealed for 1 h at 70 °C. TMPE-OH's CV is measured in 0.2 M ACN solution with a gold-coated glass as the WE. Both measurements use a Pt wire as counter electrode (CE), Ag wire as quasi reference electrode (RE), and 0.1 M Tetrabutylammonium hexafluorophosphate (TBAPF₆, > 99.0 %, Merck)/ACN (anhydrous, Fischer Scientific) as the supporting electrolyte. The measurements are calibrated to the Ferrocene (Fc/Fc⁺) redox couple and are performed in an inert environment (< 0.5 ppm O₂, < 0.5 ppm H₂O).

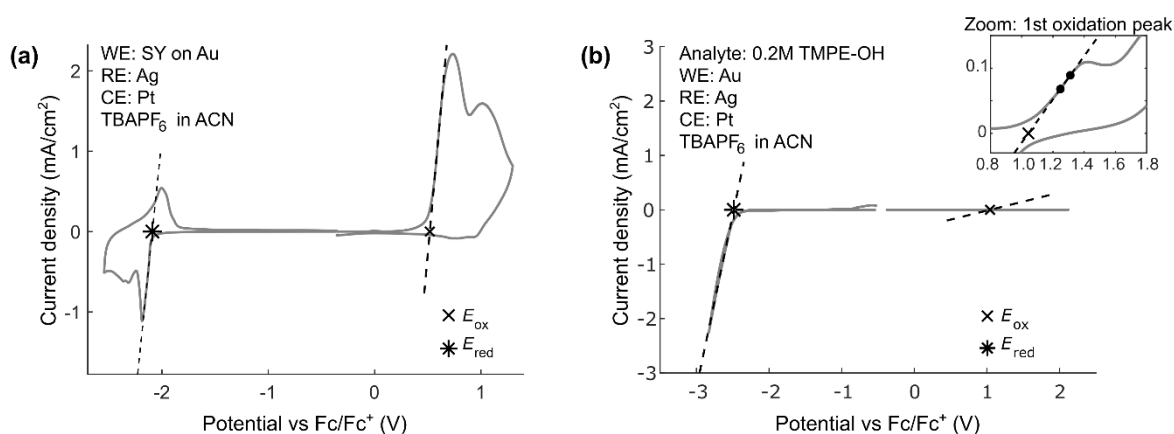


Figure S1. Cyclic voltammograms of (a) SY and (b) TMPE-OH ($M_n = 1014 \text{ g mol}^{-1}$) to extract their redox potentials.

The HOMO and LUMO levels we find are -5.3 and -2.7 eV for SY, -5.8 and -2.3 eV for TMPE-OH ($M_n = 1\text{ k g/mol}$), and -5.3 and -2.9 eV for TMPE-OH ($M_n = 450 \text{ g/mol}$). They are calculated from the voltage onset potentials derived from tangents at the half-maximum current using the relation:

$$E_{\text{HOMO/LUMO}} = -e(4.8 + E_{1/2}),$$

where E is the HOMO/LUMO level in eV, e is the fundamental electronic charge, and $E_{1/2}$ is the voltage onset potential vs. Fc/Fc⁺ in V. (J. Pommerehne, et al. "Efficient two layer leds on a polymer blend basis." *Advanced Materials* 7.6 (1995): 551-554.)

S2. Voltage-luminance turn-on transients

Figure S2 displays the turn-on characteristics during the first 10 s of operation for the three LECs (open symbols) and the D-OLED (closed squares). The pristine devices are identically fabricated as those in the main manuscript and driven at a constant current of 1 mA (corresponding to 25 mA/cm²).

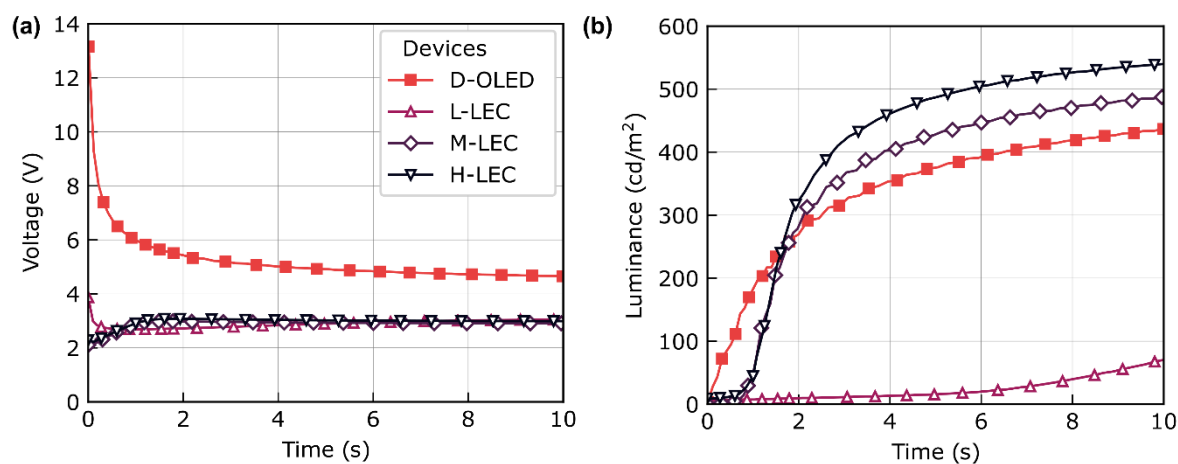


Figure S2. Temporal evolution of (a) the driving voltage and (b) the forward luminance for devices driven by a constant current of 1 mA (= 25 mA/cm²) using a voltage compliance of 21 V.

Here, we use an Agilent U2722A SMU for driving the devices. The luminance is measured with a calibrated photodiode (S9219-01, Hamamatsu Photonics) and is read by the same Agilent SMU. In contrast to the data presented in the main manuscript, Figure 2, the data acquisition is handled by a custom-made Python program, which allows us to record the voltage-luminance transients at 100 ms intervals.

S3. Capacitance density

IS measures the quantities $|Z|$ and φ , corresponding to the real and imaginary parts of Z (R and X , respectively), with i being the imaginary unit:

$$\begin{aligned}Z &= R + iX, \\R &= \operatorname{Re}(Z) = |Z| \cos(\varphi), \\X &= \operatorname{Im}(Z) = |Z| \sin(\varphi).\end{aligned}$$

The capacitance C' is defined via the admittance, the inverse of the impedance. The capacitance density $C = C'/A$ considers the pixel area A .

$$\begin{aligned}C' &= \frac{1}{\omega} \operatorname{Im}\left(\frac{1}{Z}\right) \\&= \frac{1}{\omega} \operatorname{Im}\left(\frac{1}{R + iX}\right) = \frac{1}{\omega} \operatorname{Im}\left(\frac{(R - iX)}{(R + iX)(R - iX)}\right) \\&= \frac{1}{\omega} \operatorname{Im}\left(\frac{R - iX}{R^2 + X^2}\right) = \frac{-X}{\omega|Z|^2} \\C &= \frac{C'}{A} = \frac{-X}{A \omega|Z|^2}\end{aligned}$$

S4. Equivalent circuit model (ECM) parameters

The ECM analyzes the Debye circuit displayed in the inset of Figure 3(d) in the main manuscript using LTspice. The netlist of the ECM is evaluated in a Python script using the LTspice package and running LTspice in the background. It looks as follows:

```
V1 0 N002 AC 0.02
C1 0 N002 {C1}
R1 0 N001 {R1}
C2 N001 N002 {C2}
.ac dec 10 1e-2 1e5
.end
```

V1 corresponds to the applied V_{AC} , C1 to C_{geo} , C2 to C_{EDL} , and R1 to R_{bulk} . C1 and C2 are used according to the measured values (cf. Table 2 in the main manuscript). R1 is the only fitting parameter and was chosen such that the modeled IS data resembled the experimental data.

Table S1. Parameter values used for the ECM in the main manuscript.

	N-OLED	D-OLED	L-LEC	M-LEC	H-LEC
{C1} (F)	9.14e-10	9.96e-10	1.19e-9	1.51e-9	1.60e-9
{R1} (Ω)	2e11	8e9	3e7	8e6	3e6
{C2} (F)	1.3e4	1.3e4	9.11e-8	1.27e-7	1.27e-7

The EDL capacitances (C2) of the N-OLED and D-OLED should be infinite, since they do not comprise mobile ions. As a numerical representation, we put them at extremely high values.

The full Python code is available for download. Please find the link in the main manuscript under “Data availability”.

S5. Further polar molecules as dopants

We blend four different polar organic molecules into SY, fabricate devices as in the main manuscript (ITO/SY:polar molecule/Al) with $d_{AM} = 40 (\pm 5)$ nm, and run them at a constant current of 1 mA (= 25 mA/cm²). The polar molecules are:

- TMPE-OH, $M_n \approx 450$ g/mol (Sigma-Aldrich, USA)
- TMPE-OH, $M_n \approx 1014$ g/mol (Merck, Germany)
- PEGDME: Poly(ethylene glycol) dimethyl ether, $M_n \approx 1000$ g/mol (Sigma-Aldrich, USA)
- PEG-PPG-PEG: Poly(ethylene glycol)-block-poly(propylene glycol)-block-poly(ethylene glycol), $M_n \approx 14600$ g/mol (Sigma-Aldrich, USA)

For all devices, we observe that increasing the concentration of polar molecules reduces the driving voltage. Beyond 40 wt%, the AM becomes non-uniform, the driving voltage increases again, and the devices become prone to shorts. The data of the non-functional devices is not shown for clarity.

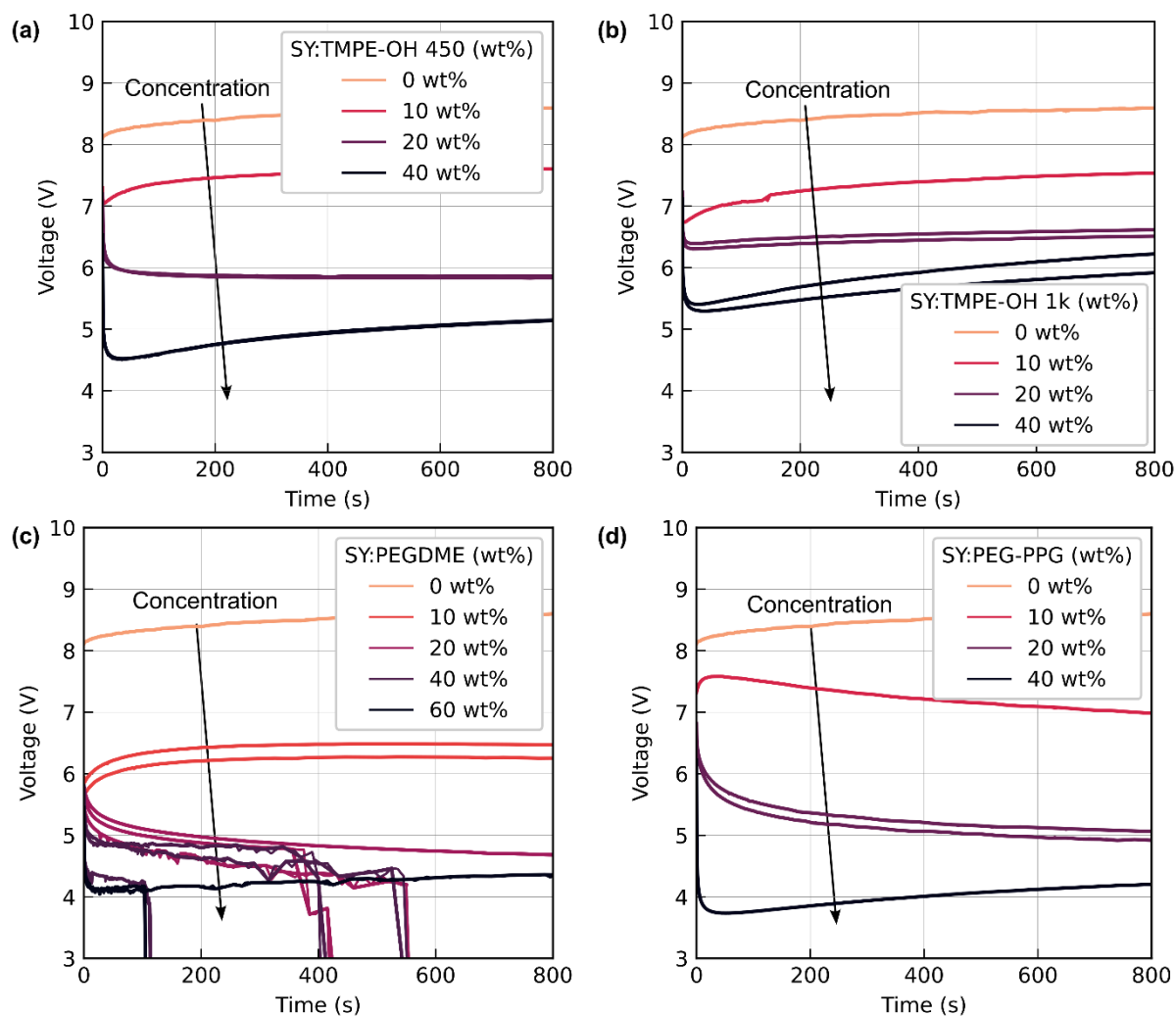


Figure S3. Dependence of the driving voltage on the concentration of (a) TMPE-OH, $M_n \approx 450$ g mol⁻¹, (b) TMPE-OH, $M_n \approx 1014$ g/mol, (c) PEGDME, and (d) PEG-PPG-PEG. The pristine devices are driven at 1 mA (= 25mA/cm²).

Now, we fabricate D-OLEDs using the above dipolar compounds and test their voltage-luminance transients compared to the N-OLED characteristics. Their film thickness is increased compared to the previous measurement to achieve bright devices, cf. Table S2.

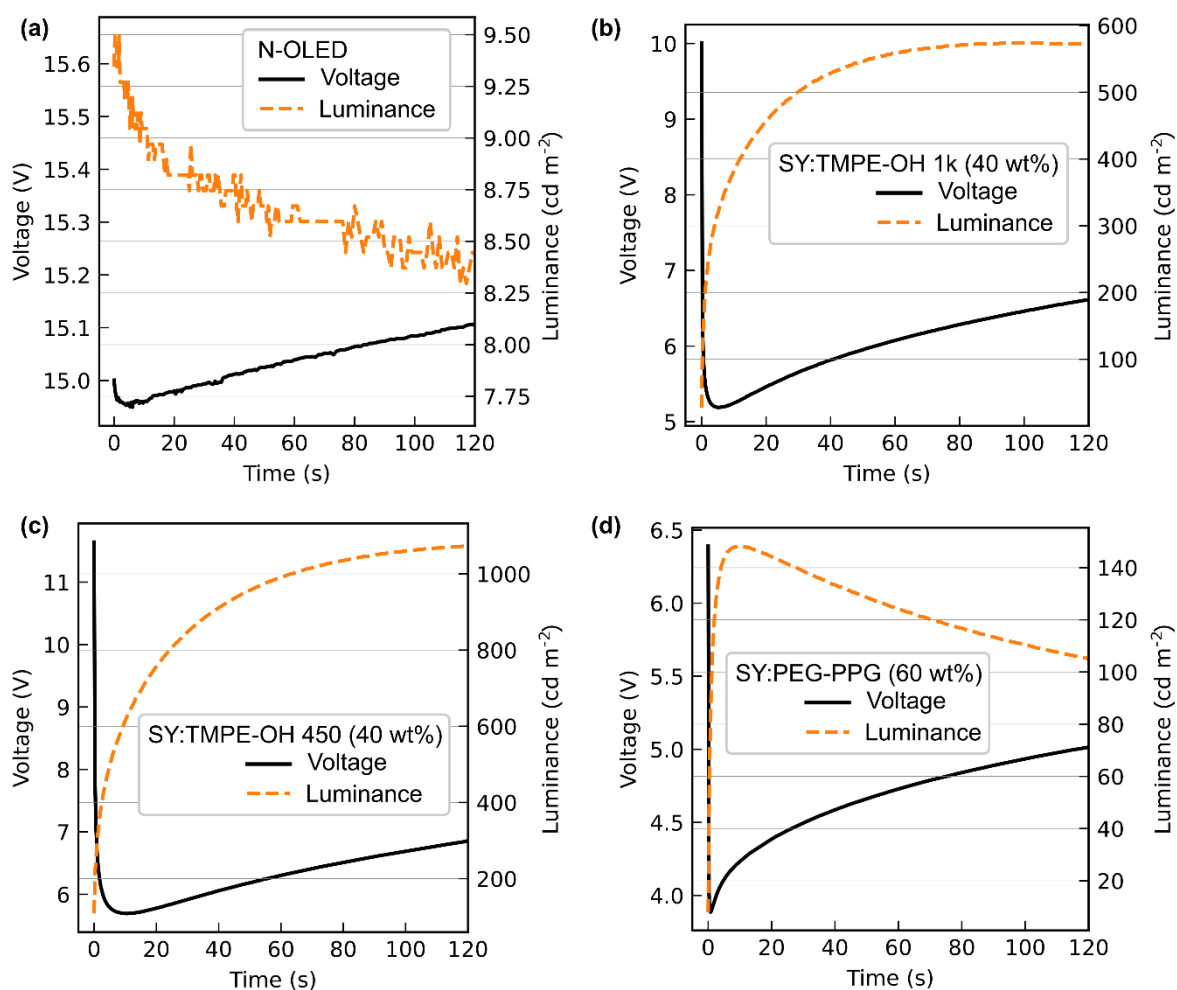


Figure S4. Voltage-luminance transients for devices driven at 0.4 mA (10 mA/cm^2). Subfigure (a) displays the N-OLED characteristics, and (b-d) contain the dipole compound indicated in the legends.

Figure S4 shows that all auxiliary dipolar compounds significantly decrease the driving voltage and increase the forward luminance, compared to the N-OLED presented in Figure S4(a).

Table S2. Active layer thickness (d_{AM}) of the devices presented in Figure S4.

Device	N-OLED	D-OLED		
		TMPE-OH 450	TMPE-OH 1k	PEG-PPG
d_{AM} (nm)	117 ± 5	132 ± 5	134 ± 5	148 ± 10

S6. Using the TADF emitter 4TCzBN instead of SY

In this experiment, we replace SY with the sky-blue thermally activated delayed fluorescence (TADF) emitter 4TCzBN and dope it with TMPE-OH ($M_n \approx 450$ g/mol) at increasing weight percentages. As observed for the SY devices (Figure S3), an increasing dipolar doping reduces the driving voltage significantly. The luminance, on the other hand, decreases with increasing TMPE-OH concentration. This reflects that the effectiveness of dipolar doping depends on the interplay of host and dopant, altering the electron and hole trap density, conductivity, and film morphology. For a small-molecule emitter, a polymer dopant like PEG-PPG-PEG may be better suited to produce homogeneous films.

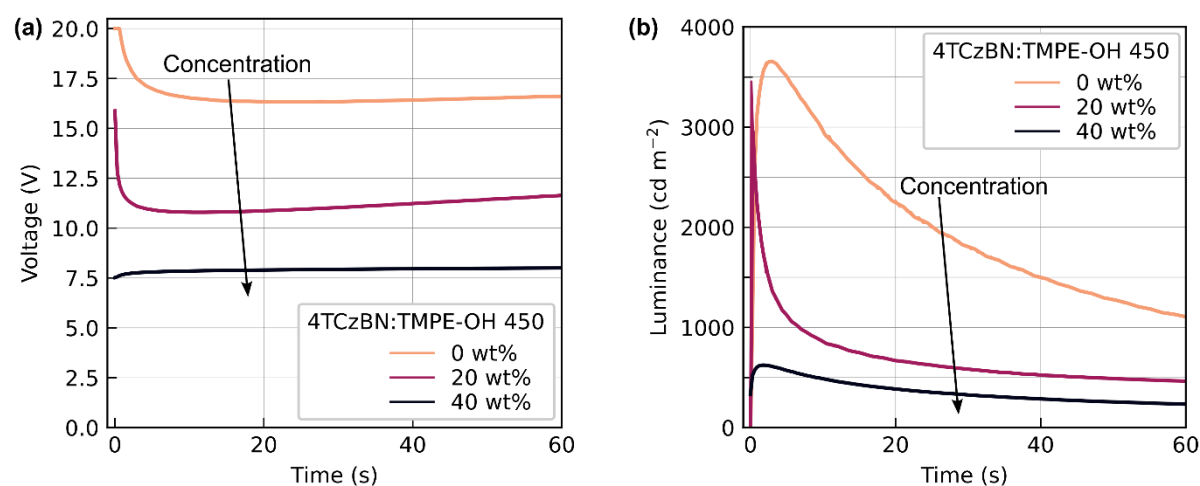


Figure S5. (a) Voltage and (b) luminance transients for ITO/AM/Al devices driven at a constant current of 1 mA (25 mA cm^{-1}). The AM consists of TMPE-OH ($M_n \approx 450$ g/mol) blended into 4TCzBN at the indicated weight percentage.

The fabrication of these devices is equivalent to the fabrication of the devices used in the main manuscript, only that SY is replaced by the TADF emitter 2,3,5,6-Tetrakis[3,6-bis(1,1-dimethylethyl)-9H-carbazol-9-yl]benzotrile (4TCzBN, Lumtec, Taiwan). This material is dried in a vacuum oven at $p < 1$ mbar and 65 °C for 24 h, dissolved in Chlorobenzene at a concentration of 40 mg/ml, and stirred at 70 °C overnight on a hotplate. The TMPE-OH ink is prepared as in the main manuscript and added according to the desired weight percentage. This AM ink is filtered with a $0.45 \mu\text{m}$ PTFE filter (VWR) and spin-coated under the same conditions as the SY devices. The d_{AM} of the dipole TADF OLEDs is displayed in Table S3. We probe the film thickness at several points close to the pixels and see that the film homogeneity (reflected by the uncertainty) decreases with increasing dipolar doping.

Table S3. AM thickness for the investigated TADF D-OLEDs consisting of 4TCzBN:TMPE-OH (x wt%).

Device	0 wt%	20 wt%	40 wt%
d_{AM} (nm)	163 ± 5	158 ± 10	145 ± 15

S7. Further impedance spectroscopy under bias

Figure S6 displays the V_{DC} -dependent impedance scans for the N-OLED, L-LEC, and H-LEC, i.e., the three devices not shown in the main manuscript. The experimental conditions are equal to the ones introduced in the main manuscript.

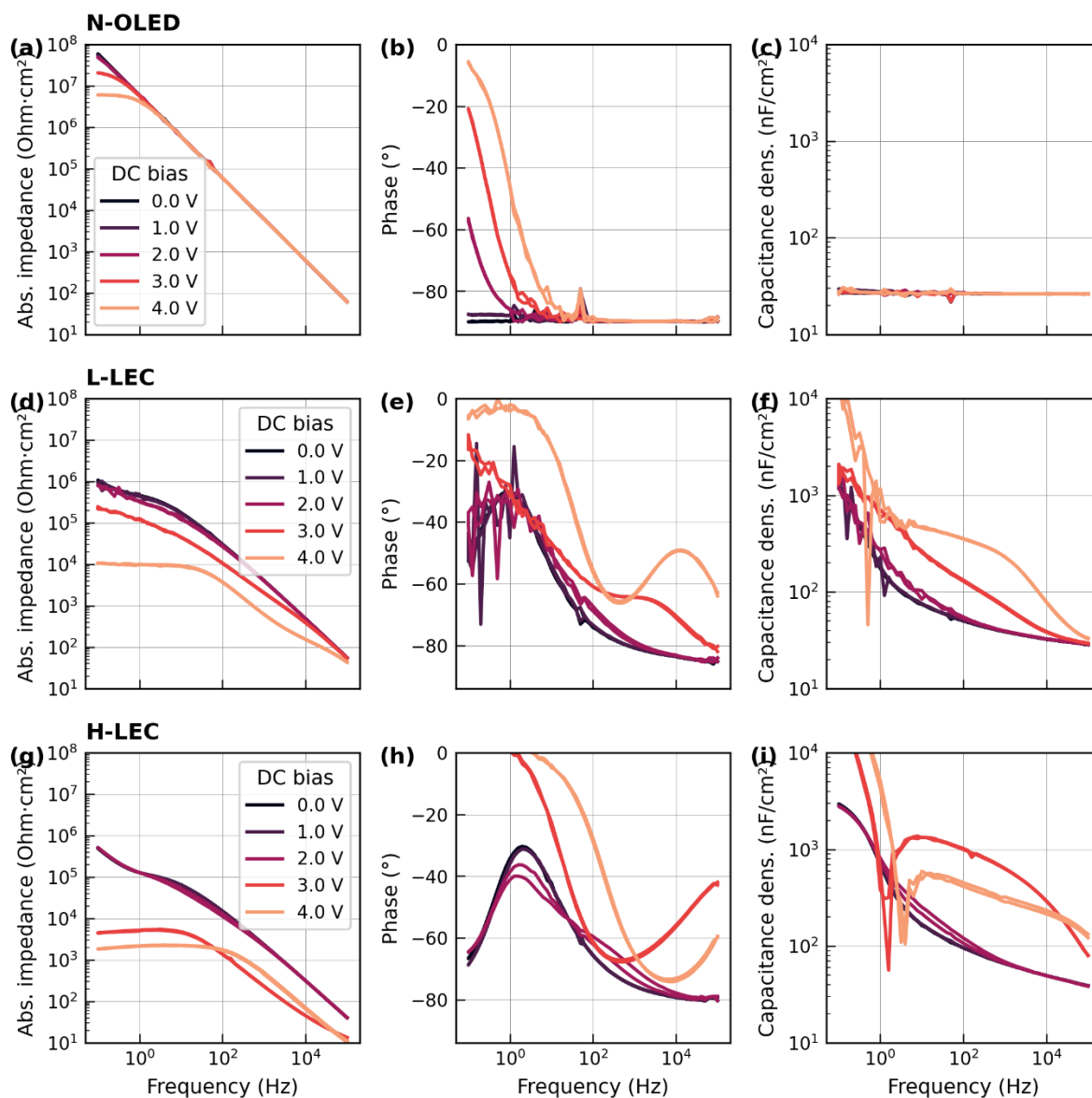


Figure S6. Voltage-dependent impedance data for (a-c) the N-OLED, (d-f) the L-LEC, and (g-i) the H-LEC. We use $V_{AC\ RMS} = 20\ mV$ and probe at $T = 25^\circ C$.